CrossMark

ORIGINAL PAPER

Spatiotemporal activities of neural network exposed to external electric fields

Hengtong Wang · Yong Chen

Abstract Neural electrical activities are due to the movement of ions in/out of the neuron and can be modulated by an external electric field. Moreover, clinical evidences reveal that the modulated activities of brain tissue by an external electric field are associated with normal or pathological brain functions. In this paper, we investigated the spatiotemporal activities of a network of neurons considering an AC electric field. It is shown that the external electric field has a significant impact on the activities of the neural network. The strong external electric field facilitates the neuron firing action potentials and enhances the mean firing rate of the network, but disrupts the synchronicity of the activities of the neural network. The information entropy revealed that the external field is capable of changing the amount of information in the neural network and the interspike internals distribution can also be changed by the external field regardless the network parameters. It is observed a v-shape resonant area in the E_{appl}-f (field intensity–field frequency) parameter space, where the neural network exhibits a high firing rate but weak synchronicity and low value of information entropy. Moreover, the effect of the electric field on the spatiotemporal activities of the neural network is detected in different connection fraction and network size. Our current work gives the insight into the effect of the external electric field on the spatiotemporal activities of the neural network.

H. Wang (✉)
College of Physics and Information Technology, Shaanxi Normal University, Xi'an 710119, China
e-mail: wanghengtong@snnu.edu.cn

Y. Chen
Center of Soft Matter Physics and its Application, Beihang University, Beijing 100191, China

Y. Chen
School of Physics and Nuclear Energy Engineering, Beihang University, Beijing 100191, China
e-mail: ychen@buaa.edu.cn

1 Introduction

Information processing in the brain is based on spatiotemporal patterns of electrical activities of neuronal networks, and it is also believed that the spatiotemporal patterns of neural activities are underlying features of many cognitive as well as pathological phenomenons [1,2]. In the last two decades, the spatiotemporal activities of neuronal networks have received much attention. It is revealed that neuronal synchronization underlies spatiotemporal pattern formation in the healthy and pathological brain [3–6]. The synchronization mechanisms have been observed in many neural process experimentally, including visual system development [7], conscious attention to stimuli [8],

movement preparation [9], and the maintenance of representations in memory [10]. The former theoretical research works also show that spatiotemporal pattern formation in neuronal networks depends on many factors including the interplay among synapses [11–14], external or intrinsic noise [15–17], network topology, and cellular properties [18,19].

Neural electrical activities are due to movement of ions across the neuronal membranes in the nervous system. It is also reported that the weak electric field has a significant effect on electrical activities of single neuron as well as neural network [20–24]. With the effect of the periodic electric field, neuron can response completed mode-locking behaviors and phase lockings as well as chaotic dynamics depending on the parameter values of the amplitude and frequency of the electric field [25]. There is also a rich bifurcation including the Hopf bifurcation, the period-adding bifurcation, and the period-doubling bifurcation [26,27]. Neurons exposed to the extremely low-frequency electric field can also change normal firing properties [26]. Introduced a external electric field, the spiral wave of a regular network of HH neurons encounters death, when the intensity of the electric field exceeds the critical threshold; otherwise, the spiral wave keeps alive completely [28].

External electric fields influence the human body just as they influence the material made up of charged particles. Extracellular electric fields exist throughout the living brain. Moreover, due to wide utilizations of power line and electric equipments, electromagnetic exposure in the environment has been nearly one hundred million times stronger than centuries before, and many nervous diseases probably caused by electromagnetic field [29,30]. Thus, it is great importance that the research on activities of neural network exposed to an external electric field.

In the current work, we extend the numerical work in this context from the firing pattern of a single neuron to the spatiotemporal activities of a network of neurons and focus on an AC external electric field. The rest of this paper arranged as follows. In Sect. 2, brief introduction of an one-compartment HH model under an electric field and simulation methods are given. Then, the simulation results are given in Sect. 3. Finally, conclusions and discussions are made in the last section.

2 Material and methods

2.1 Neuron model and external electric field

The neuron in our neural network is chosen as the Hodgkin–Huxley conductance-based model, which describes how action potentials are initiated and propagated in a single neuron [31,32]. Here, the neuron is a single-patch model, and the current along the axon is ignored. In this paper, we consider small-world neural network constructions, and the ith neuron in the network is given as follows:

$$C_m \frac{dV_i}{dt} = -g_{Na}m_i^3 h_i(V_i - E_{Na}) - g_K n_i^4(V_i - E_K)$$
$$- g_L(V_i - E_L) + I_i^{syn}(t) + \xi(t), \qquad (1)$$

$$\frac{dm_i}{dt} = \alpha_m(1 - m_i) - \beta_m m_i, \qquad (2)$$

$$\frac{dh_i}{dt} = \alpha_h(1 - h_i) - \beta_h h_i, \qquad (3)$$

$$\frac{dn_i}{dt} = \alpha_n(1 - n_i) - \beta_n n_i, \qquad (4)$$

The experimentally fited voltage-dependent transition rates are given as follows

$$\alpha_m = \frac{(0.1 - 0.01V_i)}{[\exp(1 - 0.1V_i) - 1]},$$
$$\beta_m = 0.125\exp(-V_i/80),$$
$$\alpha_h = \frac{(2.5 - 0.1V_i)}{[\exp(2.5 - 0.1V_i) - 1]},$$
$$\beta_h = 4\exp(-V_i/18),$$
$$\alpha_n = 0.07\exp(-V_i/20),$$
$$\beta_n = 1/[\exp(3 - 0.1V_i) + 1].$$

where V_i is the membrane potential of the ith neuron. m_i, h_i, and n_i represent the activation and inactivation of the sodium current and the activation of the potassium current, respectively. $C_m = 1\,\mu\text{F/cm}^2$ is the membrane capacitance. The constants $g_{Na} = 120$ mS/cm^2, $g_K = 36$ mS/cm^2, and $g_L = 0.3$ mS/cm^2 are the maximal conductances of the sodium, potassium, and leakage channels. $E_{Na} = 50$ mV, $E_K = -77$ mV, and $E_L = -54.5$ mV stand for the corresponding reversal potentials, respectively. $I_i^{syn}(t)$ is the total synaptic current of ith neuron. $\xi(t)$ is Gaussian white noise, which indicates the current noise and satisfies $\langle\xi(t)\rangle = 0$ and

$\langle \xi_i(t_1)\xi_j(t_2)\rangle = 2D\delta_{i,j}\delta(t_1 - t_2)$. D is the noise intensity and set as 2.5 mA/cm^2 in our simulation.

We use the synaptic current $I_i^{syn}(t)$ between neurons in the neural network described as follow [33]

$$I_i^{syn} = g_{syn} \sum_j^N a_{i,j} r_j (V_i - E_s). \tag{5}$$

here g_{syn} is the conductance of the synapse controlling the synaptic input amplitude, $a_{i,j}$ is the coupling constant between the two neurons i and j, which is determined by the coupling pattern of the neural network. r_j represents the fraction of bound receptors, V_i is the postsynaptic membrane potential, and $E_s = 0$ mV is the reversal potential of the excitatory synapse. The fraction of bound receptors, r_j, follows the equation

$$\frac{dr_j}{dt} = \alpha[T]_j(1 - r_j) - \beta r_j, \tag{6}$$

where $[T]_j = T_{max}H(T_0^j + \tau_{syn} - t)H(t - T_0^j)$ is the concentration of neurotransmitter released into the synaptic cleft. $\alpha = 0.94$ and $\beta = 1$ are rise and decay time constants, respectively, and T_0^j is the time at which the presynaptic neuron j fires, which happens whenever the presynaptic membrane potential exceeds a predetermined threshold value. We chose 10 mV as the threshold value in our simulation. $H()$ is the Heaviside step function.

When a external electric field is applied to the brain, charges movement can be induced in brain tissue. In this work, we consider the action of the exogenous electric fields at cellular level as a membrane voltage perturbation and introducing an additive correction term V_E for the reversal potential [26,34,35]. Thus, the Eq. 1 of the HH neuron model will then turn into:

$$\begin{aligned}
C_m \frac{dV_i}{dt} = &-g_{Na}m_i^3 h_i(V_i + V_E^i - E_{Na}) \\
&- g_K n_i^4(V_i + V_E^i - E_K) - g_L(V_i + V_E^i - E_L) \\
&+ I_i^{syn}(t) + \xi(t).
\end{aligned}$$

The term V_E^i in Eq. 7 is the induced membrane voltage perturbation of the ith neuron by an applied electric field E_{appl}. In our simulation, the neuron is considered as an single patch and the sign of V_E^i is depended on angle between the field line and the exterior normal direction of the patch of the ith neuron .

When an AC field is applied, the induced potential difference can be derived from the basic electromagnetic theory [36,37]:

$$V_E^i = 1.5RE_{appl}\sin(2\pi ft)\cos(\theta_i)/\sqrt{1 + (2\pi f\tau)^2}, \tag{7}$$

$$\tau = RC_m(\rho_{int} - \rho_{ext})/2. \tag{8}$$

where R is the cell radius (typically, on the order of 10 μm). E_{appl} is the strength of applied field, and θ_i is the angle between the field line and the exterior normal direction of the patch of the ith neuron. It is noted that the neurons in the network are supposed as uniformly distributed in the electric field. Thus, θ_i ($i = 1,2,3,...,N$) is set as uniform random numbers between 0 and 2π. $\rho_{int} = 7050$ Ωcm and $\rho_{ext} = 910$ Ωcm are the resistivity of the internal fluid and that of the external medium of the neuron, respectively .

2.2 The measurements

To quantify observed spatiotemporal patterns of network activities and distinguish various network behaviors, we introduce the population firing rate and busting synchronization of neural network.

The average frequency of network, F, was defined as the average firing rate of the whole neurons of network over the duration of the simulation run:

$$F = \frac{\sum_i^N F_i}{N}, \text{ and} \tag{9}$$

here, F_i is the firing rate of neuron i, which is defined as average spikes of neuron i in the simulation time.

We used an interspike distance synchrony measure to monitor the degree of spiking synchrony in the network. The bursting synchronization S is based on the time-ordered set of network spikes and defined as follows [17,18,38]:

$$S = \frac{1}{\sqrt{N}}\left(\frac{\sqrt{\langle\tau_v^2\rangle - \langle\tau_v\rangle^2}}{\tau_v} - 1\right) \tag{10}$$

here, τ_v is the network interspike interval corresponding to the time difference between spikes v and $v + 1$ of the network Note that the spike times do not necessarily correspond to spikes of the same neuron in the neural network.

2.3 Network connectivity and simulation method

Many studies in the past decade revealed that the structural and functional neural networks exhibit the
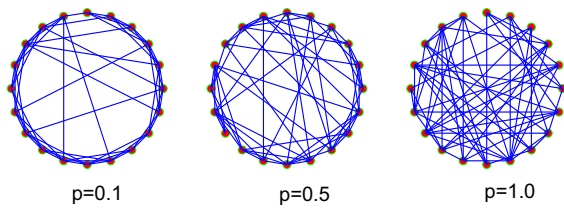
Fig. 1 Example of small-world network topologies with 20 neurons. The rewiring parameter p is set as $p = 0.1, 0.5, 1.0$ from *left* to *right*

small-world phenomenon from Caenorhabditis elegans to humans [39,40]. In this paper, the neural network was constructed using the small-world network paradigm [41]. The number of neurons in the network is set as 100. The mean connectivity fraction (the mean ratio of the number of synapse of each neuron) is set as 5 %. The rewiring parameter p is the probability of replacing a local neighbor connection with a connection randomly assigned elsewhere in the network and is set as a free parameter in this work. Figure 1 give the schematic diagram of the small-world network in this paper.

In our numerical simulation, the Box–Mueller algorithm is used with step size 0.001 ms [42]. All numerical results in the simulation are obtained by no less than 10 times averages.

3 Simulation results

3.1 Firing pattern of the neural network without external field

Firstly, the mean firing rate and bursting synchronization of neural network without external field are given in Fig. 2. For the weak synaptic conductivity, the mean firing rate of the network and the bursting synchronization of the neural network are relatively small. The neural network randomly fires few action potentials in the case of the weak synaptic conductivity. When the synaptic conductivity is strong, the firing rate of the neural network is high, especially for the network with the low rewiring probability. However, the neural network displays the best synchronous firing activities with the stronger synaptic conductivity and higher rewiring probability.

The raster plots of the firing time of each neuron are more clear to show the neural network activities.
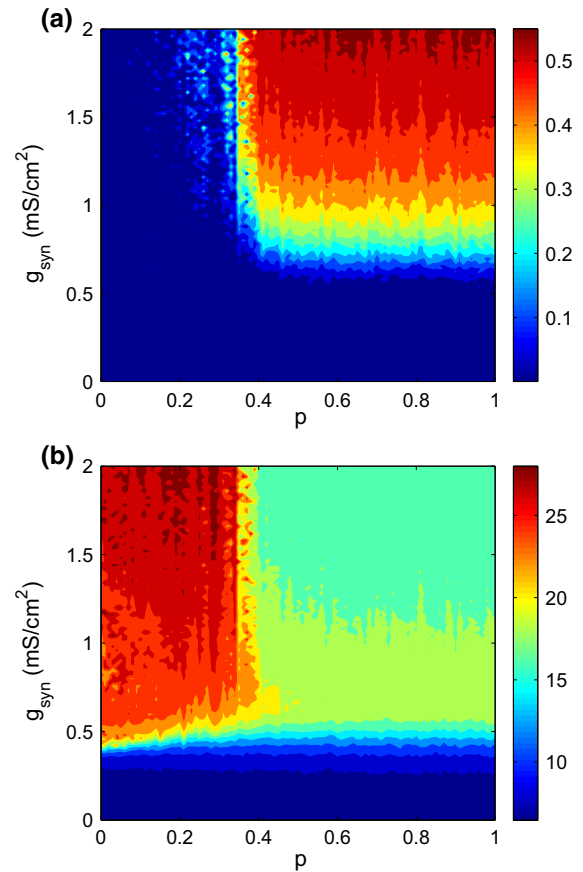

Fig. 2 The bursting synchronization (**a**) and the mean frequency (**b**) of the neural network activities as function of rewiring probability and synaptic conductivity

Figure 3 gives the raster plots of the network activities with the different synaptic conductivities and rewiring probabilities. For the weak synaptic conductivity in the top panels of Fig. 3, only few neurons in the network randomly fire action potentials and display low mean firing rate. As the synaptic conductivity is increased, the firing pattern of the network resembles the repetitive chains for the low rewiring probability. For the high rewiring probability, however, the mean firing rate of the network is also increased and the firing patterns of the network are still random. However, the neural network shows the synchronous firing pattern as the rewiring probability and synaptic conductivity are both very high (see the $g_{syn} = 1.5$ mS/cm^2, $p = 0.9$ in Fig. 3).

In a word, the network activities depend on the parameters of synaptic conductivity and rewiring probability of the neural network. Thus, in the following work,
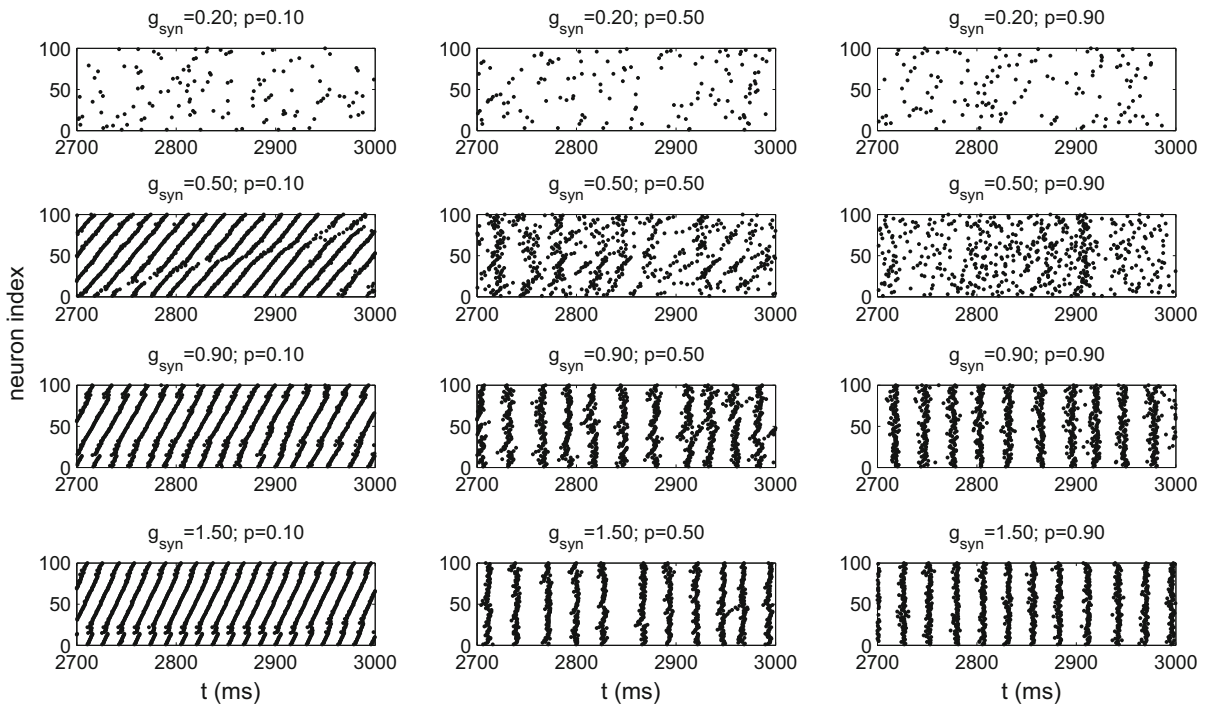
Fig. 3 The raster plots show the firing time of neurons in the network for different synaptic conductivity and rewiring probability

we choose several specific values of the synaptic conductivity and rewiring probability to simulate the effect of an external electric field on the neural network activities.

3.2 Firing frequency and synchronicity of the neural network with AC field

In this section, we consider the case of AC external electric field with sinusoidal form, which is defined by Eqs. 7 and 8. The parameters (the intensity E_{appl} and the frequency f) of the sinusoidal field are set as free parameters. Here, we choose the rewiring probability as $p = 0.1, 0.9$ and the synaptic conductivity as $g_{\text{syn}} = 0.2, 0.9$ mS/cm^2.

For the neural network with weak synaptic conductivity, the activities of the network are not synchronized, and even the intensity of the sinusoidal field is very strong. However, the firing rate of the neural network can be modified to a great extent by the external field. Figure 4 shows a color map of the bursting synchronization (upper panels) and firing rate (bottom panels) with the synaptic conductivity $g_{\text{syn}} = 0.2$ mS/cm^2. The left and right panels give the results of the neural

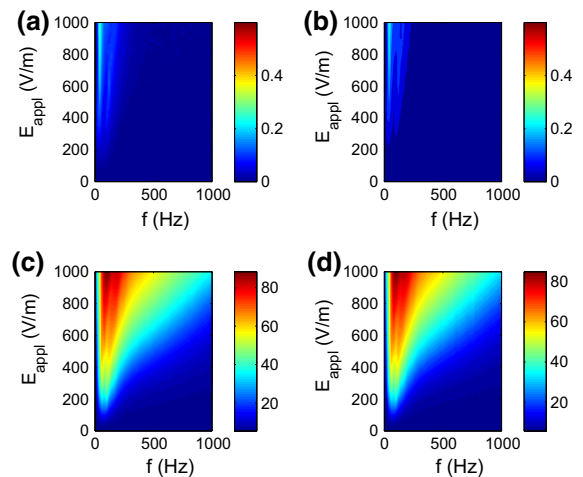**Fig. 4** Bursting synchronization (**a**, **b**) and firing rate (**c**, **d**) of the network in *color plots*. Synaptic connective is set as $g_{\text{syn}} = 0.2$ mS/cm^2. The rewiring probability $p = 0.1$ in (**a**, **c**); $p = 0.9$ in (**b**, **d**)

network with rewiring probability $p = 0.1$ and 0.9, respectively. As the parameters (the intensity E_{appl} and the frequency f) of the sinusoidal field are changed, the bursting synchronization of the network with the rewiring probability $p = 0.1$ and 0.9 is altered little and
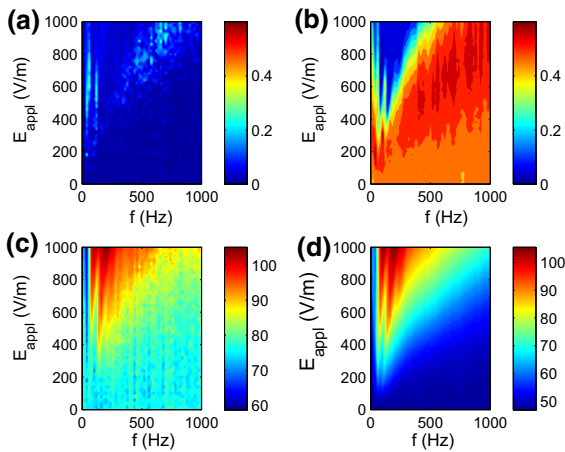
Fig. 5 Bursting synchronization (**a**, **b**) and firing rate (**c**, **d**) of the network in *color plots*. Synaptic connective is set as $g_{syn} = 0.9$ mS/cm^2. The rewiring probability $p = 0.1$ in (**a**, **c**); $p = 0.9$ in (**b**, **d**)

no more than 0.25. This result reveals that the network firing is not synchronized showing the random firing pattern. For the weak field (see as $E_{appl} < 100$ V/m in Fig. 4c, d), the firing rate of the network is similar to that without AC electric field and nearly do not change with the frequency of the AC electric field. When the intensity of the field is enhanced, the network exhibits a high firing rate, especially for the AC electric field frequency near 100 HZ. For the stronger field, the frequency range of AC electric field to induce the high firing rate is enlarged to the high-frequency direction. It is clear that the firing rate is increased with the intensity of the sinusoidal electric field. As a whole, the higher firing rate emerges in a v-shape parameter area in the E_{appl}-f panel (see as Fig. 4c, d). It is also noted that the firing patterns of the network nearly do not change the rewiring probability.

As the synaptic conductivity increased, the effect of sinusoidal field on the neural network activities is almost the same as that shown in Fig. 4, except for some little changes in the value of the bursting synchronization and firing rate. When synaptic intensity is above 0.6 mS/cm^2, the patterns of the neural network activities are very different from that of weak synaptic intensity.

As shown in Fig. 5, the color maps of the bursting synchronization (upper panels) and firing rate (bottom panels) are given as the synaptic conductivity $g_{syn} = 0.9$ mS/cm^2. For the low rewiring probability (see Fig. 5a, c), the neural network still does not

show synchronized firing activities. Moreover, the firing rate of the network nearly does not change for the weak sinusoidal electric field, but is higher than that of the neural network with weak synaptic connection. As the sinusoidal field is strong, there is also a v-shape parameter area in E_{appl}-f panel, where the neural network displays a high firing rate. For the high rewiring probability, the results are more interesting. When the parameters of the sinusoidal electric field is chosen in the v-shape area of the E_{appl}-f panel, the neural network shows the lowest bursting synchronization as shown in Fig. 5b. Outside v-shape area, however, the activity of the neural network shows very large bursting synchronization. As the intensity of a sinusoidal electric field increased, the bursting synchronization is increased outside the v-shape area. That is to say the sinusoidal electric field destroyed the synchronized neural network activities with the parameters in the v-shape area. However, the corresponding firing rate in the v-shape is higher than that outside (see in Fig. 5d). Moreover, the firing rate of the neural network also increases with the intensity of the external field.

As the firing response of neural network show in Figs. 4 and 5, there is very high-frequency response in the v-shape parameter area. In the presence of a sinusoidal electric field and background noise, a single neuron displays stochastic resonance when the field parameters are chosen in the v-shape area. Although neurons are coupled into a complex network, the mean frequency response is still very high. This collective behavior also reveals a novel resonant phenomenon of neural network exposed in a periodic electric field. It is noted that such resonant phenomenon is robust to coupling topology.

The typical raster plots of the neural network exposed to the sinusoidal electric field are given in Fig. 6. For the weak synaptic conductivity ($g_{syn} = 0.2$ mS/cm^2), neurons in the neural network (with the rewiring probability $p = 0.1$ or $p = 0.9$) almost randomly fire action potentials. For strong synaptic conductivity, the activity patterns of the neural network took the form repetitive chains (as $p = 0.1$, $E_{appl} = 200$ mS/cm^2, $f = 100$ Hz in Fig. 6). When the parameters of the sinusoidal field belong to the v-shape area in the E_{appl}-f panel, the neurons in the network fire large number of action potentials asynchronously, whereas the firing activities of the network show synchronous behaviors with the parameters outside of the v-shape area (as $p = 0.9$; $E_{appl} = 600$; $f = 700$ in Fig. 6).
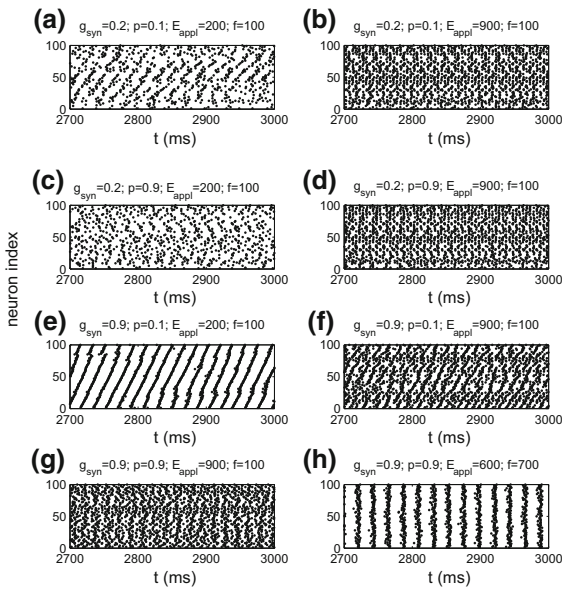
Fig. 6 The raster plots show the firing time of neurons in the neural network exposed to sinusoidal electric field

Fig. 7 Information entropy of the neural network exposed to a sinusoidal electric field. The parameters are set as: **a** $g_{syn} = 0.2$ mS/cm^2 and $p = 0.2$; **b** $g_{syn} = 0.2$ mS/cm^2 and $p = 0.9$; **c** $g_{syn} = 0.9$ mS/cm^2 and $p = 0.2$; and **d** $g_{syn} = 0.9$ mS/cm^2 and $p = 0.9$. The number of neurons in the network is set as 100. The mean connectivity fraction (the mean ratio of the number of synapse of each neuron) is set as 5 %

3.3 Information entropy of the neural network with AC field

The results of the above sections show that the external electric field has a significant impact on the activities of the neural network. In this section, we focus on the changes in the transmission information of the neural network in the presence of the external AC filed. To do this, we introduced the information entropy H to measure the amount of information in the network [43,44]. Information entropy is a concept from information theory. The definition of the information entropy of a neural network is given by

$$H = -\frac{1}{N} \sum_{i=1}^{N} \sum_{\text{observe}\Delta t} P_{\text{ISI}}^{i}(\Delta t) \log_2 \left(P_{\text{ISI}}^{i}(\Delta t) \right). \tag{11}$$

Here, N is the total neuron number of the neural network. $P_{ISI}^i(\Delta t)$ is the probability of ISIs of ith neuron. Δt was chosen as 1.0 ms. Information entropy tells how much information there is in an event and has applications in many areas, including statistical inference, biology, machine learning, and so on. This information entropy can serve as order parameter to give us not only the amount of information in the neural network, but also property of the neural network activities.
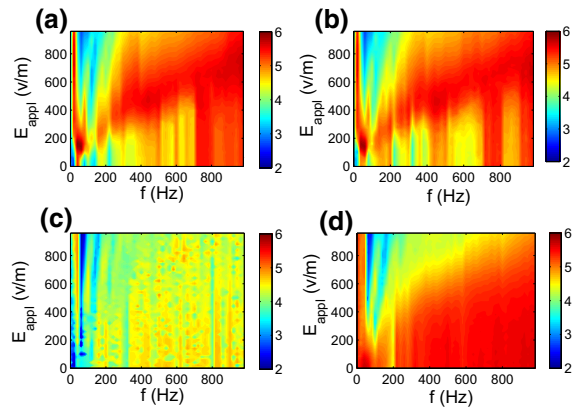
Figure 7 gives the information entropy of the neural network exposed to a sinusoidal electric field. When the synaptic conductivity is weak, the external field has a little effect on the synchronicity of the neural network firing. However, the external field shows a significant impact on the information entropy of the neural network. As shown in Fig. 7a, b, the neural network exhibits high value of information entropy in the most region of the E_{appl}-f parameter space. That is due to the fact that external field enhances irregularity of the neural network firing, when the synaptic conductivity is weak. That is also the reason that the firing of neural network is not synchronous.

As the synaptic conductivity is increased, the effect of an external field on the information entropy become weak, when the rewiring probability of the network work is low. As shown in Fig. 7c, the value of information entropy is relatively lower than that of the neural network with weak synaptic conductivity. In this case, the neural network still exhibits irregular firing and the interspike intervals of the neural network is distributed in a scattered area, although the external field enhances the firing of the neural network and the strong synaptic conductivity enhances the communication between neurons. That is why the neural network still does not show synchronous firing, but high firing frequency (as shown in Fig. 5a, c). When the synaptic intensity and the rewiring probability are both large enough, the infor-

mation entropy in the E_{appl}-f parameter space exhibits similar pattern to that of bursting synchronization (see in Fig. 5d). There is a distinct v-shape parameter area in E_{appl} -f panel, where the neural network displays a small value of information entropy. Outside this v-shape area, however, the neural network shows a larger value of information entropy.

It is also noted that the neural network displays a small value of information entropy as the frequency of the external field in the region 0–300 Hz regardless the synaptic conductivity and the rewiring probability. In this region, the neural network also shows the highest firing frequency. Those results reveal that resonance of the neural network for the external field is in this frequency region. Interestingly, the previous work reveals that the application of low-frequency (0–300 Hz) time-varying external magnetic fields induces currents affecting neural firing in the central nervous system and affects pain sensitivity in snails, rodents, and humans. This frequency region is the same as the resonance frequency region in our simulation.

3.4 The effect of the connectivity fraction and network size

As the results of the previous studies, spatiotemporal activities of the neural network depend on the overall synaptic input of individual neuron as well as the number of cells in the neural network [18,38]. Thus, we consider the spatiotemporal activities of neural network with different connectivity fraction and network size in the sinusoidal electric field.

Firstly, we only change the number of the neurons in the neural network, keeping the connectivity fraction as the default value ($k = 0.05$). As shown in Fig. 8, the bursting synchronization and mean firing rate of the network with different number of neurons are given as functions of the frequency of the sinusoidal electric field. When the frequency of the external field is low, the bursting synchronization fluctuates largely both of the networks with low and high rewiring probability. Increasing the frequency of the electric field, the bursting synchronization of the network with the low rewiring probability is increased and then decreased with the frequency of the electric field. For the network with high rewiring probability, however, the bursting synchronization is increasing with the frequency of the
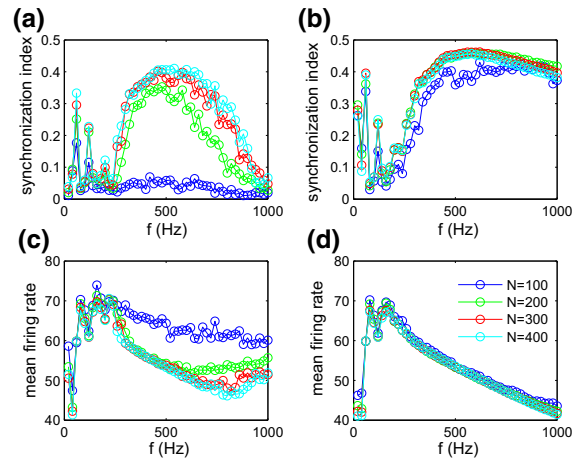

Fig. 8 Effect of the number of neurons in the network. The intensity of the external field $E_{appl} = 700$ V/m and the synaptic conductivity $g_{syn} = 0.9$ mS/cm^2. *Left panels $p = 0.2$; right panels $p = 0.9$. Upper panels* give the results of the bursting synchronization; *bottom panels* give the results of mean firing rate of the network

external field, and then decreases in the high-frequency area. It is interesting that the network with a larger number of neurons exhibits larger bursting synchronization. This result reveals that the network with a larger number of neurons exhibits more synchronous firing pattern. Moreover, the network with large number of neurons could display synchronous firing pattern as the frequency of external field near 500 Hz, which does not depend on the rewiring probability (see as Fig. 8a, b).

As shown in Fig. 8c, d, the mean firing rate of the neural network is increased with the frequency of external field, when the frequency of the external field is low. As the frequency of the external field is high enough (nearly over the 200 Hz), the mean firing rate of the network begins to decrease. For the low rewiring probability, the network with a larger number of neurons displays lower mean firing rate. For the high rewiring probability, however, the number of neurons in the network almost has no effect on the mean firing rate of the network.

In Fig. 9, we change the connectivity fraction and set the network size as the default value ($N = 100$). As the frequency of the external field increasing, the changing trends of the bursting synchronization and mean firing rate are similar to that showed in Fig. 8. The neural network with higher connectivity fraction displays the better synchronous firing pattern. Moreover, the firing
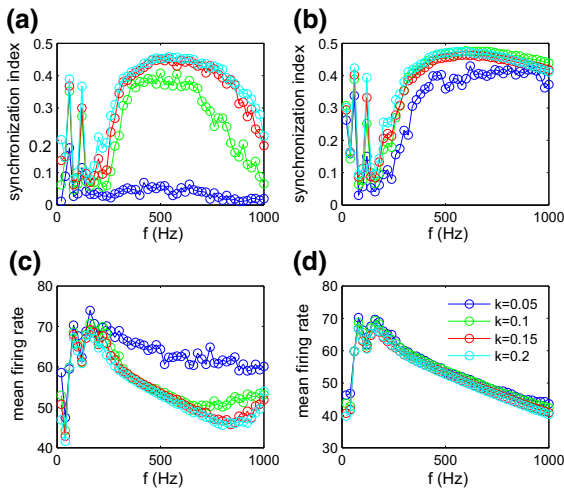
Fig. 9 Effect of the mean connectivity fraction of the neural network. The intensity of the external field $E_{appl} = 700$ V/m and the synaptic conductivity $g_{syn} = 0.9$ mS/cm^2. *left panels* $p = 0.2$; *right panels* $p = 0.9$. *Upper panels* give the results of the bursting synchronization; *bottom panels* give the results of mean firing rate of the network

rate of the neural network with low rewiring probability decreases as the connectivity fraction increases in the high- frequency area of the external field. However, the firing rate of the network with high rewiring probability has a little change when the connectivity fraction increased.

4 Conclusion and discussion

In this paper, we investigated the spatiotemporal activities of neural network exposed to an external electric fields. We observed that the neural network exhibited intriguing behaviors as a result of interaction among network structure, synaptic conductivity, and the electric fields. The weak external field does not change the activities of neural network regardless the form of the external field, the network structure, and the synaptic conductivities. However, the strong external field has significant effects on the activities of neuron: not only changed the mean firing rate but also modified the firing synchronicity of the neural network.

For the AC electric field, the neural network exhibits more interesting spatiotemporal activities. When the synaptic conductivity is weak, the synchronicity of the neural network is similar to that without the AC field and nearly does not change by changing the field para-

meters. When the synaptic intensity is strong, the synchronicity of the neural network is modulated by the external electric field to a large extent. However, the mean response frequency of the network almost not depends on synaptic conductivity and rewiring probability. The information entropy revealed that the external field is capable of changing the amount of information in the neural network. Moreover, the interspike internals distribution can also be changed by the external regardless the network parameters. In the E_{appl}-f parameter space, there is a v-shape area, where the neural network exhibits a high firing rate. For the neural network with higher rewiring probability and stronger conductivity, it is interesting that the neural network displays asynchronous firing in the v-shape parameter area, but the neural network exhibits better synchronous firing pattern outside this area. The collective behaviors of the neurons reveal a novel resonant phenomenon of neural network exposed in a periodic electric field.

As the neuron network exposed to the sinusoidal electric field with high enough frequency, we also observed that the synchronicity of the neural network could be enhanced and the mean firing rate could be decreased as the number of the neuron and the connection fraction of the neural network increases in the case of network with low rewiring probability. When the neural network has a high rewiring probability, however, the synchronicity (as well as the firing rate) of the neural network with different network size (as well as connectivity fraction) is nearly the same.

Nowadays, everyone, both at home and at work, is exposed to a complex mix of weak electric and magnetic fields in the environment due to the abundant manmade electromagnetic fields. Electric fields influence the human body by the electromagnetic force on the charged particles in the human body. It is also reported that there exists a strong relationship between some diseases and the electric field [45]. Here, we studied the spatiotemporal activities of neural network exposed in an electric field. Our results reveal that the weak electric field does not change the spatiotemporal activities of neural network, but the strong electric field does. Those results conform to the common sense and may be helpful to the theoretical studies of the effects of electric field on the human brain. A potential implication of this research helps neuroscientist and neurosurgeon to choose a proper external electric field to control the activities of a network of neurons or brain tissues. It is

also reported the electric field had been used to control epileptic seizure-like events in hippocampal brain slices [46]. Our current results can also reveal that the mechanism of this method to control epileptic seizure-like events is based on the disturbance on the hyper-synchronous brain activities.

However, the real nervous system is a highly complex system, and the electromagnetic field cannot only change the balance of charged particles and has heating effect in the human body. Thus, further studies on the effect of the electromagnetic field to the human brain are needed in both theory and experiment.

Appendix

Description of the neuronal model

The neuron in our neural network is chosen as the Hodgkin–Huxley conductance-based model, which describes how action potentials are initiated and propagated in a single neuron. Here, the neuron is treated as a single-patch model, and the current along the axon is ignored. To make the model closely match the real nervous system, the angle (θ) between the field line and the exterior normal direction of the patches has a uniform distribution, based on the complex structure neural network and neurons.

On the other hand, we consider the action of the exogenous electric fields at the cellular level as a membrane voltage perturbation and introducing an additive correction term V_E for the reversal potential. In fact, the external fields interact with the ions in the neuron and induce a reset of the distribution of ions both inside and outside membranes. Thus, the reversal potential should be modified. Based on the theory of the electric field (induced by ion distribution) force just balances the diffusion force at equilibrium, in the current model, we suppose that force induced by an external electrical field V_E is balanced by the changes in distribution of ions. Thus, the final reversal potential E_{ion}^{final} (with effect of an external field) can be simply written as: $E_{ion}^{final} = -V_E + E_{ion}$. Here, E_{ion} is the reversal potential without of an external field.

References

1. Ahlfors, S.P., Simpson, G.V., Dale, A.M., Belliveau, J.W., Liu, A.K., Korvenoja, A., Virtanen, J., Huotilainen, M., Tootell, R.B.H., Aronen, H.J., Ilmoniemi, R.J.: Spatiotemporal activity of a cortical network for processing visual motion revealed by MEG and fMRI. J Neurophysiol. **82**, 2545–2555 (1999)
2. Gerstner, W., Kistler, W.M.: Spiking Neuron Models: Single Neurons, Populations, Plasticity, 1st edn. Cambridge University Press, Cambridge (2002)
3. Varela, F., Lachaux, J., Rodriguez, E., Martinerie, J.: The brainweb: phase synchronization and large-scale integration. Nat. Rev. Neurosci. **2**, 229–239 (2001)
4. Roelfsema, P.R., Engel, A., König, P., Singer, W.: Visuomotor integration is associated with zero time-lag synchronization among cortical areas. Nature **385**, 157–161 (1997)
5. Bressler, S.: Interareal synchronization in the visual cortex. Behav. Brain Res. **76**, 37–49 (1996)
6. Rodriguez, E.: Perceptions shadow: long-distance synchronization of human brain activity. Nature **397**, 430–433 (1999)
7. Foster, D.J., Wilson, M.A.: Reverse replay of behavioural sequences in hippocampal place cells during the awake state. Nature **440**, 680–683 (2006)
8. Melloni, L., Molina, C., Pena, M., Torres, D., Singer, W., Rodriguez, E.: Synchronization of neural activity across cortical areas correlates with conscious perception. J. Neurosci. **27**, 2858–2865 (2007)
9. Riehle, A., Grün, S., Diesmann, M., Aertsen, A.: Spike synchronization and rate modulation differentially involved in motor cortical function. Science **278**, 1950–1953 (1997)
10. Axmacher, N., Mormann, F., Fernández, G., Elger, C.E., Fell, J.: Memory formation by neuronal synchronization. Brain Res. Rev. **52**, 170–182 (2006)
11. Turrigiano, G.G., Nelson, S.B.: Homeostatic plasticity in the developing nervous system. Nat. Rev. Neurosci. **5**, 97–107 (2004)
12. Liu, Y., Zhang, L.I., Tao, H.W.: Heterosynaptic scaling of developing GABAergic synapses: dependence on glutamatergic input and developmental stage. J. Neurosci. **27**, 5301–5312 (2007)
13. Ledoux, E., Brunel, N.: Dynamics of networks of excitatory and inhibitory neurons in response to time-dependent inputs. Front. Comput. Neurosci. **5**, 25 (2011)
14. Ma, J., Song, X., Jin, W., Wang, C.: Autapse-induced synchronization in a coupled neuronal network. Chaos Solitons Fractals **80**, 31–38 (2015)
15. Gong, Y., Xie, Y., Lin, X., Hao, Y.: Non-gaussian noise-optimized intracellular cytosolic calcium oscillations. BioSystems. **103**, 13–17 (2011)
16. Zhang, R., Hou, Z., Xin, H.: Effects of non-Gaussian noise near supercritical Hopf bifurcation. Phys. A **390**, 147–153 (2011)
17. Tiesinga, P.H.E., Fellous, J.M., Salinas, E., José, J.V., Sejnowski, T.J.: Synchronization as a mechanism for attentional gain modulation. Neurocomputing **58–60**, 641–646 (2004)
18. Bogaard, A., Parent, J., Zochowski, M., Booth, V.: Interaction of cellular and network mechanisms in spatiotempo-

ral pattern formation in neuronal networks. J. Neurosci. **29**, 1677–1687 (2009)

19. Xu, B., Gong, Y., Wang, L., Wu, Y.: Multiple synchronization transitions due to periodic coupling strength in delayed Newman–Watts networks of chaotic bursting neurons. Nonlinear Dyn. **72**, 79–86 (2013)

20. Bikson, M., Inoue, M., Akiyama, H., Deans, J.K., Fox, J.E., Miyakawa, H., Jefferys, J.G.R.: Effects of uniform extracellular DC electric fields on excitability in rat hippocampal slices in vitro. J. Physiol. **557**, 175–190 (2004)

21. Radman, T., Su, Y., An, J.H., Parra, L.C., Bikson, M.: Spike timing amplifies the effect of electric fields on neurons: implications for endogenous field effects. J. Neurosci. **27**, 3030–3036 (2007)

22. McCaig, C.D., Song, B., Rajnicek, A.M.: Electrical dimensions in cell science. J. Cell Sci. **122**, 4267–4276 (2009)

23. Robertson, J.A., Théberge, J., Weller, J., Drost, D.J., Prato, F.S., Thomas, A.W.: Low-frequency pulsed electromagnetic field exposure can alter neuroprocessing in humans. J. R. Soc. Interface. **7**, 467–473 (2010)

24. Dogru, A.G., Tunik, S., Akpolat, V., Dogru, M., Saribas, E.E., Kaya, F.A., Nergiz, Y.: The effects of pulsed and sinusoidal electromagnetic fields on E-cadherin and type IV collagen in gingiva: a histopathological and immunohistochemical study. Adv. Clin. Exp. Med. **22**, 245–252 (2013)

25. Che, Y.Q., Wang, J., Si, W.J., Fei, X.Y.: Phase-locking and chaos in a silent Hodgkin–Huxley neuron exposed to sinusoidal electric field. Chaos Solitons Fractals **39**, 454462 (2009)

26. Yi, G.S., Wang, J., Han, C.X., Deng, B., Wei, X.: Spiking patterns of a minimal neuron to ELF sinusoidal electric field. Appl. Math. Model. **36**, 3673–3684 (2012)

27. Che, Y., Wang, J., Deng, B., Wei, X., Han, C.: Bifurcations in the Hodgkin–Huxley model exposed to DC electric fields. Neurocomputing **81**, 41–48 (2012)

28. Wang, C., Ma, J., Jin, W.Y., Wu, Y.: Electric Field-induced dynamical evolution of spiral wave in the regular networks of Hodgkin–Huxley neurons. Appl. Math. Comput. **218**, 4467–4474 (2011)

29. Stuchly, M.A., Dawson, T.W.: Interaction of low-frequency electric and magnetic fields with the human body. Proc. IEEE **88**, 643–664 (2000)

30. Johansen, C.: Electromagnetic fields and health effects-epidemiologic studies of cancer, diseases of the central nervous system and arrhythmia-related heart disease. Scand. J. Work Environ Health. **30**(Suppl 1), 1–30 (2004)

31. Hodgkin, A.L., Huxley, A.F.: A quantitative description of membrane current and its application to conduction and excitation in nerve. J. Physiol. (Lond.) **117**, 500–544 (1952)

32. Shilnikov, A.: Complete dynamical analysis of a neuron model. Nonlinear Dyn. **68**, 305–328 (2011)

33. Balenzuela, P., Garca-Ojalvo, J.: Role of chemical synapses in coupled neurons with noise. Phys. Rev. E. **72**, 021901 (2005)

34. Kotnik, T., Miklavčič, D., Slivnik, T.: Time course of transmembrane voltage induced by time-varying electric fields a method for theoretical analysis and its application. Bioelectrochem. Bioenerg. **45**, 3–16 (1998)

35. Gianni, M., Liberti, M., Apollonio, F., DInzeo, G.: Modeling electromagnetic fields detectability in a HH-like neuronal system: stochastic resonance and window behavior. Biol. Cybern. **94**, 118–127 (2006)

36. Doruk, R.O.: Control of repetitive firing in Hodgkin–Huxley nerve fibers using electric fields. Chaos Solitons Fractals **52**, 66–72 (2013)

37. Marszalek, P., Liu, D.S., Tsong, T.Y.: Schwan equation and transmembrane potential induced by alternating electric field. Biophys. J. **58**, 1053–1058 (1990)

38. Fink, C.G., Booth, V., Zochowski, M.: Cellularly-driven differences in network synchronization propensity are differentially modulated by firing frequency. PLoS Comput. Biol. **7**, e1002062 (2011)

39. Bullmore, E., Sporns, O.: Complex brain networks: graph theoretical analysis of structural and functional systems. Nat. Rev. Neurosci. **10**, 186–198 (2009)

40. Stam, C.J.: Modern network science of neurological disorders. Nat. Rev. Neurosci. **10**, 186–198 (2014)

41. Watts, D.J., Strogatz, S.H.: Collective dynamics of small-world networks. Nature **393**, 440–442 (1998)

42. Fox, R.F., Gatland, I.R., Roy, R., Vemuri, G.: Fast, accurate algorithm for numerical simulation of exponentially correlated colored noise. Phys. Rev. A. **38**, 5938–5940 (1988)

43. Abarbanel H.D.I., Tumer, E.C. Reading neural encodings using phase space methods, perspectives and problems in nonlinear science. In: Kaplan E, Marsden JE, Sreenivasan KR (eds) A Celebratory Volume in Honor of Lawrence Sirovich, Springer Applied Mathematical Sciences Series. Springer, Berlin (2003)

44. Wang, H., Wang, L., Yu, L., Chen, Y.: Response of Morris–Lecar neurons to various stimuli. Phys. Rev. E. **83**, 021915 (2011)

45. Van der Mark, M., Vermeulen, R., Nijssen, P.C.G., Mulleners, W.M., Sas, A.M.G., van Laar, T., Kromhout, H., Huss, A.: Extremely low-frequency magnetic field exposure, electrical shocks and risk of Parkinsons disease. Int. Arch. Occup. Environ. Health. **88**, 227–234 (2015)

46. Li, Y., Mogul, D.J.: Electrical control of epileptic seizures. J. Clin. Neurophysiol. **24**, 197–204 (2007)